Journal of Biomaterials Applications
http://jba.sagepub.com/

In Vivo Assessment of Bone Ingrowth Potential of Three-Dimensional E-Beam Produced Implant Surfaces and the Effect of Additional Treatment by Acid Etching and Hydroxyapatite Coating

J. Elizabeth Biemond, Gerjon Hannink, Annemarijn M. G. Jurrius, Nico Verdonschot and Pieter Buma

J Biomater Appl 2012 26: 861 originally published online 27 January 2011
DOI: 10.1177/0885328210391495

The online version of this article can be found at:
http://jba.sagepub.com/content/26/7/861

Published by:
SAGE
http://www.sagepublications.com

In Vivo Assessment of Bone Ingrowth Potential of Three-Dimensional E-Beam Produced Implant Surfaces and the Effect of Additional Treatment by Acid Etching and Hydroxyapatite Coating

J. ELIZABETH BIEMOND,[1,*] GERJON HANNINK,[1] ANNEMARIJN M. G. JURRIUS,[1] NICO VERDONSCHOT[1,2] AND PIETER BUMA[1]

[1]*Orthopaedic Research Laboratory, Radboud University Nijmegen Medical Center, PO Box 9101, 6500 HB Nijmegen, The Netherlands*

[2]*Laboratory for Biomechanical Engineering, University of Twente, PO Box 217 7500 AE Enschede, The Netherlands*

ABSTRACT: The bone ingrowth potential of three-dimensional E-beam-produced implant surfaces was examined by histology and compared to a porous plasma-sprayed control. The effects of acid etching and a hydroxyapatite (HA) coating were also evaluated by histology. Specimens were implanted in the distal femur of 10 goats. Histological analysis of bone ingrowth was performed 6 weeks after implantation. The E-beam-produced surfaces showed significantly better bone ingrowth compared to the plasma-sprayed control. Additional treatment of the E-beam surface structures with a HA coating, further improved bone ingrowth potential of these structures significantly. Acid etching of the E-beam structures did not influence bone

*Author to whom correspondence should be addressed.
E-mail: l.biemond@orthop.umcn.nl
Figures 1–3 and 5–7 appear in color online: http://jba.sagepub.com

0885-3282/12/07 0861–15 $10.00/0 DOI: 10.1177/0885328210391495

ingrowth significantly. In conclusion, the HA-coated, E-beam-produced structures are promising potential implant surfaces.

KEY WORDS: bone ingrowth, E-beam, hydroxyapatite, acid etching, surface characterization, *in vivo*.

INTRODUCTION

Although total hip arthroplasty is a very successful orthopedic procedure, 5–10% of the cementless implants still fail within 10 years of implantation, mainly due to aseptic loosening [1,2]. The frequency of failure is likely to increase due to the implantation in younger and more active patients [3].

The long-term success of cementless prostheses depends on fixation by bone ingrowth in the early postoperative period [4]. Bone ingrowth is influenced by the implant surface characteristics, such as pore size and porosity. Although the optimal pore size has yet to be determined, it is evident that this parameter too affects bone ingrowth [5]. It has been shown that a substantial increase in fixation strength can be obtained by increasing the porosity of implants to 75–80% [6]. Furthermore, interconnectivity between the pores is crucial in order to permit bone ingrowth [7]. Bone ingrowth into a porous structure might increase the strength at the bone–implant interface. However, one can expect that ingrowth beyond a certain depth does not enhance the strength of the bone–implant interface, similar as seen for the cement–bone interface [8].

Electron beam melting is a rapid-prototyping technique that can be utilized to produce a solid implant and a porous surface structure in one manufacturing step. The implant is built up out of metal powder to reproduce a geometry defined by a three-dimensional (3D) computer-aided design (CAD) model [9,10]. Therefore, it is possible to design implant surfaces with many different surface characteristics. By adapting the surface characteristics, bone ingrowth could be further enhanced, resulting in better bone ingrowth than conventional implant surfaces.

Several (post-production) implant surface modifications are investigated in an attempt to improve bone ingrowth, including application of a calcium phoshpate coating (e.g., hydroxyapatite (HA)) and texturing by chemical etching [11]. HA has been applied on porous implant surfaces in order to enhance the bone ingrowth potential [12,13]. The process of bone formation onto HA-coated implants might be mediated by dissolution of the coating soon after implantation followed by the

formation of a carbonated calcium phosphate layer and bone growth toward the implant [14].

Acid etching of the surface has been shown to enhance the bone ingrowth potential of porous implant surfaces [15]. The topography of an etched implant relies on acid mixture, etching time, temperature, and topography prior to etching [11]. However, the treatment results in relatively low roughness values [16,17].

The goal of this study was to evaluate the bone ingrowth potential of three new E-beam-produced structures and to compare this to a highly porous titanium plasma spray coating. Furthermore, the influence of addition of HA and acid etching was tested.

MATERIALS AND METHODS

Specimens

The specimens ($8 \times 4 \times 10\,mm^3$, Eurocoating Spa, Trento, Italy) were produced by electron beam melting. In this rapid prototyping process, the implants were built up out of Ti6Al4V powder. The powder size used in the E-beam process ranged from 45 to 100 μm. The E-beam specimens were created using a 3D CAD model which was segmented into layers of 0.1 mm in order to generate layer information. Subsequently, a homogeneous powder layer was applied on the process platform in a vacuum chamber at constant high temperature (±700°C). The electron beam scanned the powder layer line by line and melted the loose powder particles at programmed locations forming a compact layer in the desired shape. The process platform was then lowered by one layer thickness (0.1 mm) and a new powder layer (of 0.1 mm thickness) was applied after which the process is repeated [9,10]. Upon completion, all specimens were sandblasted with corundum and cleaned in a specific washer for medical devices.

Three different 3D E-beam surface structures were developed; the gyroid structure, the star small structure, and the cubic enlarged structure. The design of the gyroid structure is based on the mathematical gyroid surface (infinitely connected periodic surface containing no straight lines). The star structure consisted of 3D cross-shapes and the cubic enlarged structure had large quadrangular pores (Figure 1). As a control, a highly porous titanium plasma spray coating (Ti sponge) and a plain, rough E-beam surface with HA coating (Osprovit®, Eurocoating Spa, Trento, Italy) were tested (Figure 2).

To evaluate the effect of further treatment of the E-beam structures, an acid-etching procedure (with a mixture of nitric and fluoridic acid

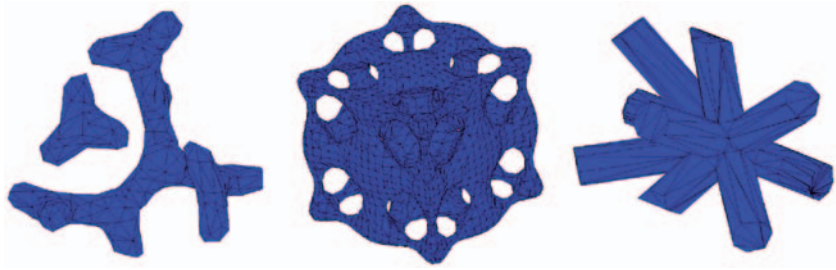

Figure 1. CAD files.
Note: The CAD files of the elements forming the gyroid, cubic enlarged, and star E-beam structures (from left to right).

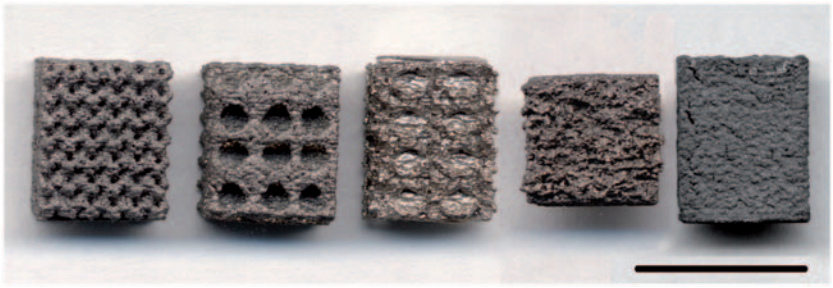

Figure 2. 3D E-beam structures.
Note: From left to right: gyroid, cubic enlarged, and star E-beam structure, the Ti sponge and rough HA surfaces. Bar = 10 mm.

solutions) was performed on the gyroid and star small structures. For the star small structure, only the etched form was tested; for the gyroid structure, an untreated surface was tested as well. Furthermore, the cubic enlarged structure was tested with and without a HA coating (applied by plasma spray technique, coating thickness $70 \pm 10\,\mu m$). All surfaces and their treatments are given in Table 1.

Two different surfaces were combined on one specimen except for the titanium plasma-sprayed sponge coating, resulting in four different specimens.

Surface Characterization

MicroCT analysis (SCANCO Medical, Switzerland, resolution 50 μm) was performed to define the pore size, porosity, pore connectivity, and surface area of each specimen. Surface roughness values of the

Table 1. Surfaces: the 3D surface structure, production process, and additional treatment of the tested surfaces.

Surface	Structure	E-beam produced	Additional treatment
Gyroid	Gyroid	Yes	None
Cubic enlarged	Cubic enlarged	Yes	None
Gyroid etched	Gyroid	Yes	Etching
Star etched	Star	Yes	Etching
Cubic enlarged HA	Cubic enlarged	Yes	HA
Rough HA	None	Yes	HA
Ti sponge	Plasma spray coating	No	None

specimens were determined using a Universal Surface Tester (UST; Innowep, Wurzburg, Germany).

Experimental Design

Surgery was performed on 10 female, skeletal mature goats (*Capra Hircus Sana*), weighing 49–67 kg (mean 55 kg). The specimens were implanted in the trabecular bone of the distal femur. Each goat received two specimens; one in the medial and one in the lateral condyl of the right leg. The different implants were equally divided among the goats and implantation areas ($n = 5$ for each group).

The goats were anesthetized with propofol (4 mg/kg B. Brown, Melsungen, Germany), intubated and anesthesia was maintained using isoflurane. The goats were placed in a lateral position and the implantation procedure was performed under strict sterile conditions. The knee was approached lateral, visualizing the origin of the lateral collateral ligament. Approximately, 1.5 cm from the origin a hole (Ø4.0 mm) was drilled reaching into the medial condyle. Saline was used during the drilling to prevent heat induced necrosis. Sharp osteotomes with increasing size ($4 \times 4\,mm^2$ to $4 \times 8\,mm^2$) were used to shape the hole to the size of the specimen. The implantation area was inspected to guarantee the specimen would be completely surrounded by trabecular bone. Just above the origin of the lateral collateral ligament a second implantation area was created (in the lateral condyl). The specimens were inserted press-fit into the holes and the facia and skin were closed separately with resorbable sutures.

The goats received ampicillin (7.5 mg/kg Intervet, Boxmeer, The Netherlands) for 4 days after surgery. Fluorochromes were administered by subcutaneous injection at 2 (Calcein green, 25 mg/kg), 4 (Xylenol orange, 30 mg/kg), and 6 weeks (Tetracyclin, 25 mg/kg) after surgery

during two consecutive days in order to generate ingrowth data of different time points for each animal. Goats were sacrificed 6 weeks postoperative by an overdose of barbiturate pentobarbital (Euthesate, Ceva Santa Animale, Libourne, France). This study was approved by the Animal Ethics Committee of the Radboud University, Nijmegen.

Histological Analysis

After sacrificing the animals, the distal femurs were retrieved. The specimens with the surrounding bone tissue were fixated in phosphate-buffered 4% formaldehyde solution for 4 days and embedded in MMA. Slices of 40 μm, perpendicular to the length of the specimen, were cut using a sawing microtome (SP 1600, Leitz, Wetzlar, Germany). Quantitative analysis of bone ingrowth was performed using fluorescence microscopy on unstained slices and light microscopy on Hematoxylin/Eosin (HE) stained slices. Each slice was analyzed using specialized software (AnalySIS 3.2 Soft Imaging System, Münster, Germany). Bone ingrowth depth was measured at 2, 4, and 6 weeks using the fluorescence microscopy. A line was drawn from the deepest fluorochrome label to the outline of the specimen. The direct bone–implant contact (BIC) was determined by the linear extent of direct bone apposition divided by the total surface perimeter of the implant.

The thickness of the coating on the cubic enlarged HA surface and rough HA surface was measured on 10 slices.

Statistical Analysis

Statistical analysis was performed with a one-way ANOVA and a LSD *post hoc* test using SPSS (16.0, SPSS Inc., Chicago, USA). A p-value less than 0.05 was considered significant.

RESULTS

Surface Characterization

The pore size of the E-beam-produced surfaces ranged from 0.40 to 1.35 mm. All E-beam-produced surfaces had a relatively high porosity (44–73%). The titanium sponge control had a pore size of 0.23 mm and a porosity of 34%. All surfaces had a good pore connectivity index and a large surface area (Table 2). The surface morphology before implantation showed the characteristic appearances of E-beam surfaces without additional treatment (a and b), with additional treatment (acid-etched

Table 2. Surface characteristics: the pore size (mm), porosity (%), pore connectivity (mm^{-3}), and surface area (mm^2) of the tested surfaces.

Surface	Pore size (mm)	Porosity (%)	Pore connectivity (mm^{-3})	Surface area (mm^2)
Gyroid	0.40	44	2.71	328
Cubic enlarged	1.35	73	1.73	239
Gyroid etched	0.47	61	4.52	306
Star etched	0.67	70	0.82	169
Cubic enlarged HA	1.23	61	0.65	297
Ti sponge	0.23	34	6.35	423

and HA-coated surfaces (c, d and e, f, respectively) and the titanium plasma-sprayed control (g) (Figures 3 and 4).

The roughness measurements showed that the roughness decreased after the etching treatment and increased after application of a HA coating (Table 3).

Histomorphometric Analysis

One Ti sponge specimen was implanted too close to the intercondylar notch and was not surrounded by trabecular bone. Therefore, this specimen was excluded for further analysis. Histological analysis of the specimens showed no sign of infection or metal debris (Figure 5).

The cubic enlarged surface structure and the cubic enlarged HA surface showed the best bone ingrowth depth. Bone ingrowth depth of the cubic enlarged structure was significantly greater compared to the gyroid (at 4 and 6 weeks, $p = 0.01$ and $p = 0.002$, respectively) and the Ti sponge surface (at 2, 4, and 6 weeks, $p = 0.03$, $p = 0.003$, and $p = 0.002$, respectively; Figure 6).

With respect to percentage direct bone implant contact, the cubic enlarged HA, rough HA, and cubic enlarged surface scored the best. The percentage direct bone implant contact was significantly better for the cubic enlarged structure than for the gyroid structure ($p = 0.03$). Coating with HA significantly increased the bone implant contact of the cubic enlarged structure ($p = 0.01$). This cubic enlarged HA surface was significantly better compared to the Ti sponge control ($p < 0.001$). The rough HA surface showed significantly higher bone implant contact than the gyroid structure ($p < 0.001$) and the Ti sponge surface ($p = 0.001$). No significant effect of chemical etching on bone implant contact was seen, although both etched surface structures showed a low amount of bone implant contact (Figure 7).

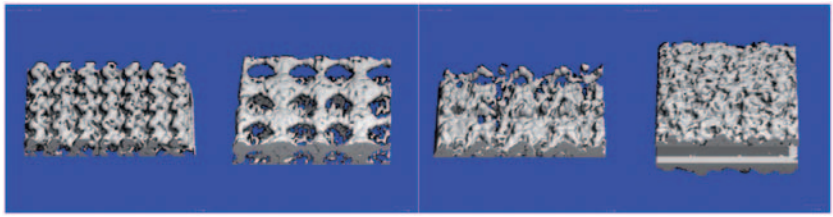

Figure 3. MicroCT images.
Note: From left to right: gyroid, cubic enlarged, star, and Ti sponge surfaces.

The thickness of the HA coating after 6 weeks of implantation was 61.6 μm (±10.7) for the cubic enlarged HA surface and 64.3 μm (±10.5) for the rough HA surface.

DISCUSSION

In this study, the bone ingrowth potential of E-beam-produced surface structures were compared to a Ti plasma spray coating with similar porosity. Furthermore, the effect of additional treatment, HA, and chemical etching was investigated.

This experiment was limited to surface characterization and histological analysis. No tests for mechanical strength of the bone implant interface were performed. Although many implant surfaces were evaluated with a limited amount of goats, the choice of the surfaces implicated some restrictions. In some cases, it was not clear whether the effect on bone ingrowth was caused by the E-beam structure or by the additional treatment. The surface characterization by microCT analysis is limited by the resolution, which means that pores under 50 μm cannot be detected. This will affect the measurements on the Ti sponge surface the most, due to the design of the surface (with the smallest pores). The absence of weight bearing in the model is a limitation of this study as well.

The cubic enlarged surface showed a significant better bone ingrowth compared to the gyroid structure and Ti sponge surface. No additional treatment was used for all these surfaces. Therefore, one could say that differences in bone ingrowth potential between these surfaces are due to either the E-beam technology itself or the surface characteristics. Comparable results of the E-beam gyroid structure and Ti sponge (with similar pore size and porosity), made clear that the E-beam technology itself does not benefit or harm the bone ingrowth potential. The superior bone ingrowth of the cubic enlarged structure compared to the gyroid

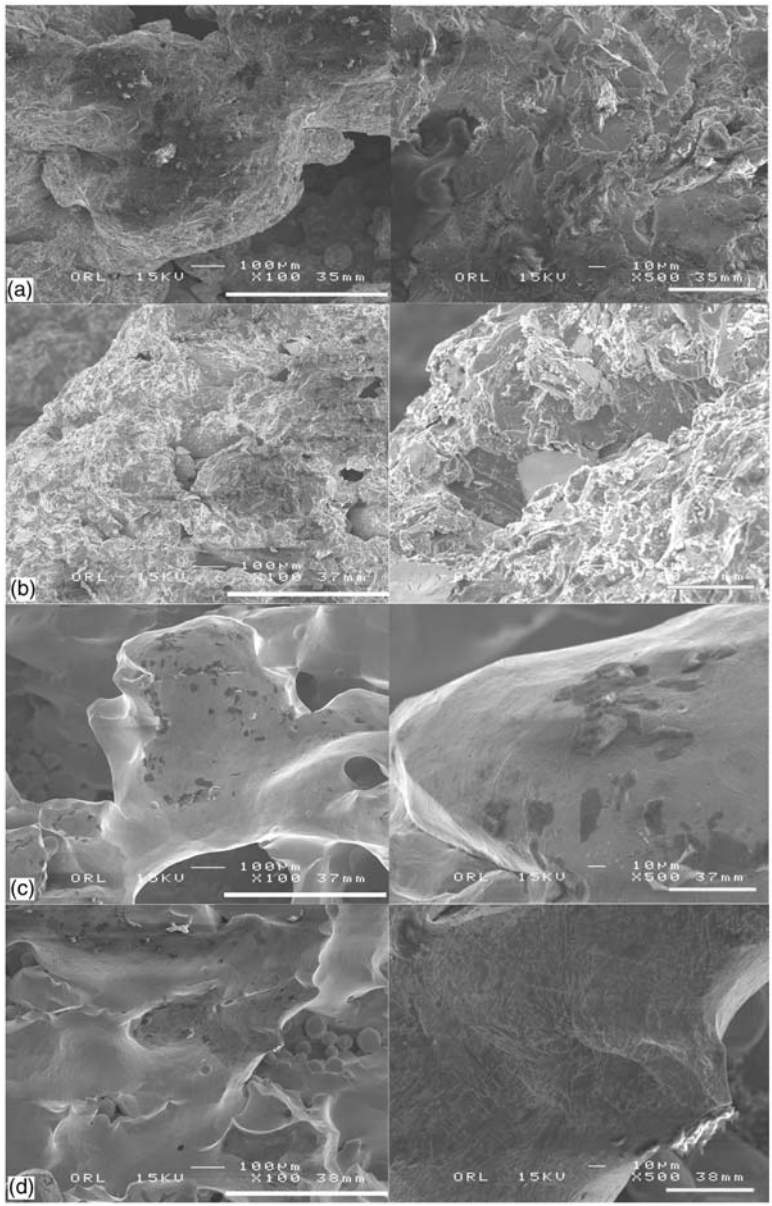

Figure 4. Surface characterization: SEM images of the gyroid (a), cubic enlarged (b), gyroid etched (c), star etched (d), cubic enlarged HA (e), rough HA (f), and Ti sponge (g) implant surfaces.
Note: Left column: bar = 500 μm, right colomn: bar = 50 μm.

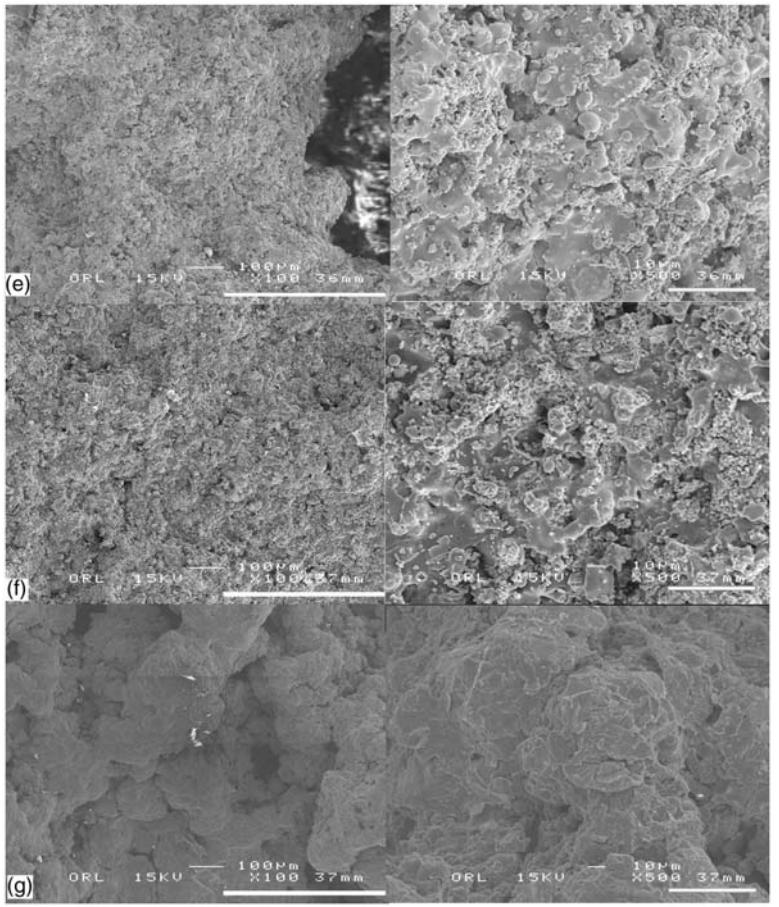

Figure 4. Continued.

Table 3. Surface roughness, R_a (μm) of the tested surfaces.

Surface	Roughness, R_a (μm)
Gyroid	3.92
Cubic enlarged	4.43
Gyroid etched	3.34
Star etched	5.62
Cubic enlarged HA	4.52
Rough HA	4.39

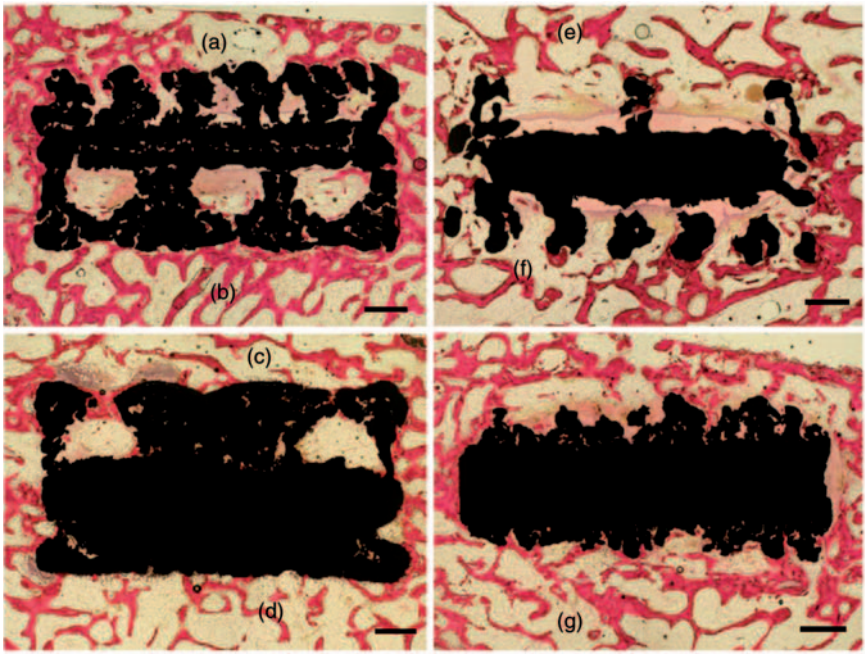

Figure 5. Histomorphology: microscopic images of histology slides of gyroid (a), cubic enlarged (b), cubic enlarged HA (c), rough HA (d), star etched (e), gyroid etched (f), and Ti sponge (g) implant surfaces. Bar = 1 mm.

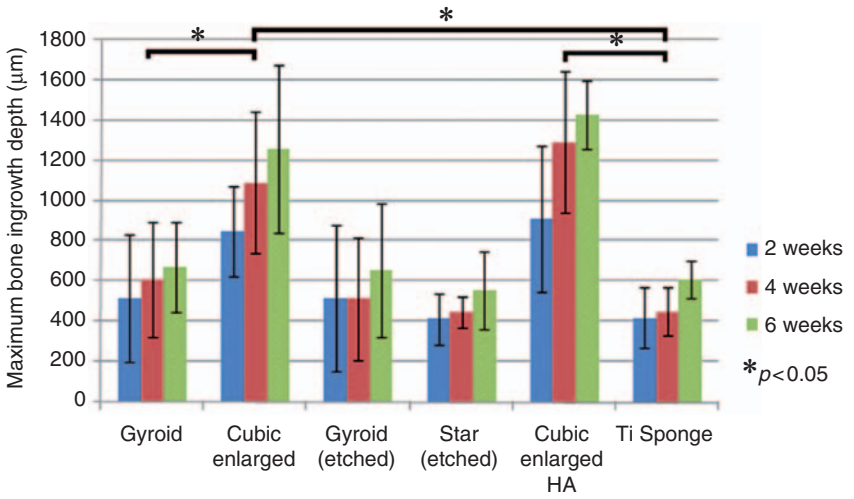

Figure 6. Bone ingrowth depth.
Note: Graph showing bone ingrowth depth for the different implant surfaces at 2, 4, and 6 weeks after surgery. Significance is indicated by*.

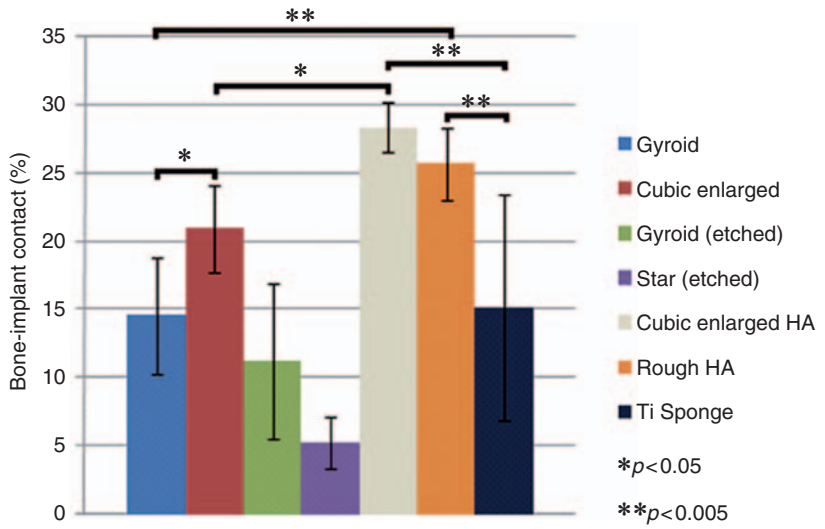

Figure 7. Bone implant contact.
Note: Graph showing the percentage of bone implant contact for the different implant surfaces. $^{*}p < 0.05$ and $^{**}p < 0.005$.

structure is therefore likely to be caused by its surface topography. This structure has a large pore size (1.35 mm) and a high porosity (73%). So, there is a clear beneficial effect of large pore size and high porosity on the bone ingrowth potential, which is supported by the literature [6,18]. Recently, various authors have showed that besides porosity, pore interconnectivity is a critical factor for bone ingrowth [7,19]. However, Otsuki et al. [7] found no differences in vascularization between two groups with different interconnectivities and suggested that the number of interconnections is a more important factor compared to the size of the interconnections. Nevertheless, no clear influence of the amount of interconnections, as determined by microCT analysis, on the amount of bone ingrowth could be concluded from this study.

Concerning the effect of additional treatments, HA significantly increased the bone ingrowth potential of a porous E-beam structure. This enhancement in bone ingrowth was visible in the early post-operative period, suggesting that HA accelerates bone ingrowth as well. The acceleration of bone ingrowth achieved by the HA coating could be beneficial with regard to postoperative partial weight-bearing and rehabilitation [20]. The fact that HA enhances and accelerates bone ingrowth when applied on implant surfaces is well known [12–14,21].

However, in this study, both these positive effects are achieved with a plasma spray technique on a porous surface.

No beneficial effect of the etching procedure on bone ingrowth could be found. This is in contrast to other studies [11,15]. This difference could be explained by the fact that in our study, the acid etching was performed on a 3D surface structure. Furthermore, as explained earlier, the success of acid etching is influenced by acid mixture, etching time, and temperature [11]. However, although the acid-etching procedure did not enhance bone ingrowth, the procedure did not harm the bone ingrowth as well.

CONCLUSION

In conclusion, the E-beam technique provides the ability to promote enhanced bone ingrowth compared to a porous, conventionally made control specimen. Additional treatment of the 3D E-beam implant surface structures with a HA coating (applied by plasma spray technique), further improves the bone ingrowth potential of these structures. Acid etching of the E-beam structures did not influence bone ingrowth.

ACKNOWLEDGMENTS

This study is cosponsored by Provincia Autonoma di Trento and Eurocoating SpA, Trento, Italy which designed and manufactured all the surfaces. The authors thank Pierfrancesco Robotti, Emanuele Magalini, and Giacomo Bianchi (Eurocoating, Trento, Italy) who actively participated in developing this study. The authors thank Willem van de Wijdeven and Léon Driessen for their technical assistance and the staff of the Central Animal Facility of the Radboud University Nijmegen for their assistance in the animal experiments.

REFERENCES

1. Eskelinen, A., Remes, V., Helenius, I., Pulkkinen, P., Nevalainen, J. and Paavolainen, P. Uncemented Total Hip Arthroplasty for Primary Osteoarthritis in Young Patients: A Mid-to Long-Term Follow-up Study from the Finnish Arthroplasty Register, *Acta Orthop.*, 2006: **77**: 57–70.
2. Karrholm, J., Garellick, G. and Herberts, P. (2007). Annual Report 2006. Swedish National Hip Arthroplasty Register.
3. McAuley, J.P., Szuszczewicz, E.S., Young, A. and Engh, C.A. Sr. Total Hip Arthroplasty in Patients 50 Years and Younger, *Clin. Orthop. Relat. Res.*, 2004: **418**: 119–125.

4. Basarir, K., Erdemli, B., Can, A., Erdemli, E. and Zeyrek, T. Osseointegration in Arthroplasty: Can Simvastatin Promote Bone Response to Implants? *Int. Orthop.*, 2009: **33**: 855–859.
5. Karageorgiou, V. and Kaplan, D. Porosity of 3D Biomaterial Scaffolds and Osteogenesis, *Biomaterials*, 2005: **26**: 5474–5491.
6. Bobyn, J.D., Stackpool, G.J., Hacking, S.A., Tanzer, M. and Krygier, J.J. Characteristics of Bone Ingrowth and Interface Mechanics of a New Porous Tantalum Biomaterial, *J. Bone Joint Surg. Br.*, 1999: **81**: 907–914.
7. Otsuki, B., Takemoto, M., Fujibayashi, S., Neo, M., Kokubo, T. and Nakamura, T. Pore Throat Size and Connectivity Determine Bone and Tissue Ingrowth into Porous Implants: Three-Dimensional Micro-CT Based Structural Analyses of Porous Bioactive Titanium Implants, *Biomaterials*, 2006: **27**: 5892–5900.
8. Majkowski, R.S., Bannister, G.C. and Miles, A.W. The Effect of Bleeding on the Cement-Bone Interface. An Experimental Study, *Clin. Orthop. Relat. Res.*, 1994: **299**: 293–297.
9. Heinl, P., Rottmair, A., Körner, C. and Singer, R. Cellular Titanium by Selective Electron Beam Melting, *Adv. Eng. Mater.*, 2007: **9**: 360–364.
10. Heinl, P., Muller, L., Korner, C., Singer, R.F. and Muller, F.A. Cellular Ti-6Al-4V Structures with Interconnected Macro Porosity for Bone Implants Fabricated by Selective Electron Beam Melting, *Acta Biomater.*, 2008: **4**: 1536–1544.
11. Daugaard, H., Elmengaard, B., Bechtold, J.E. and Soballe, K. Bone Growth Enhancement In Vivo on Press-Fit Titanium Alloy Implants with Acid Etched Microtexture, *J. Biomed. Mater. Res. Part A*, 2008: **87**: 434–440.
12. Barrere, F., van der Valk, C.M., Meijer, G., Dalmeijer, R.A., de Groot, K. and Layrolle, P. Osteointegration of Biomimetic Apatite Coating Applied onto Dense and Porous Metal Implants in Femurs of Goats, *J. Biomed. Mater. Res. Part B*, 2003: **67**: 655–665.
13. Tsukeoka, T., Suzuki, M., Ohtsuki, C. et al. Enhanced Fixation of Implants by Bone Ingrowth to Titanium Fiber Mesh: Effect of Incorporation of Hydroxyapatite Powder, *J. Biomed. Mater. Res. Part B*, 2005: **75**: 168–176.
14. Sun, L., Berndt, C.C., Gross, K.A. and Kucuk, A. Material Fundamentals and Clinical Performance of Plasma-Sprayed Hydroxyapatite Coatings: A Review, *J. Biomed. Mater. Res.*, 2001: **58**: 570–592.
15. Hacking, S.A., Harvey, E.J., Tanzer, M., Krygier, J.J. and Bobyn, J.D. Acid-Etched Microtexture for Enhancement of Bone Growth into Porous-Coated Implants, *J. Bone Joint Surg. Br.*, 2003: **85**: 1182–1189.
16. Silva, T.S., Machado, D.C., Viezzer, C., Silva Junior, A.N. and Oliveira, M.G. Effect of Titanium Surface Roughness on Human Bone Marrow Cell Proliferation and Differentiation: An Experimental Study, *Acta Cir. Bras.*, 2009: **24**: 200–205.
17. Stöver, M., Renke-Gluszko, M., Schratzenstaller, T. et al. Microstructuring of Stainless Steel Implants by Electrochemical Etching, *J. Mater. Sci.*, 2006: **41**: 5569–5575.

18. Lopez-Heredia, M.A., Goyenvalle, E., Aguado, E. et al. Bone Growth in Rapid Prototyped Porous Titanium Implants, *J. Biomed. Mater. Res. Part A*, 2008: **85**: 664–673.
19. Jones, A.C., Arns, C.H., Hutmacher, D.W., Milthorpe, B.K., Sheppard, A.P. and Knackstedt, M.A. The Correlation of Pore Morphology, Interconnectivity and Physical Properties of 3D Ceramic Scaffolds with Bone Ingrowth, *Biomaterials*, 2009: **30**: 1440–1451.
20. Habibovic, P., Barrère, F., van Blitterswijk, C.A., de Groot, K. and Layrolle, P. Biomimetic Hydroxyapatite Coating on Metal Implants, *J. Am. Ceram. Soc.*, 2002: **85**: 517–522.
21. Davis, J.R. (2005). Coatings, In: Davis & Associates (ed.), *Handbook of Materials for Medical Devices*, Novelty, Ohio, ASM International, pp. 179–194.